Interference Analysis for LoRa Chirp Spread Spectrum Signals

Brody Dunlop[†], Ha H. Nguyen[†], R. Barton[‡] and J. Henry[‡]
[†] University of Saskatchewan
57 Campus Dr., Saskatoon, SK, Canada S7N 5A9
brody.dunlop@usask.ca, ha.nguyen@usask.ca
[‡] Cisco Systems Inc.
88 Queens Quay West, Suite 2900, Toronto, ON, Canada M5J 0B8
robbarto@cisco.com, jerhenry@cisco.com

***Abstract*—LoRa modulation is a modulation scheme patented by SemTech that uses chirp spread spectrum (CSS) signals to modulate data. This paper analyzes the interference between those signals for different spreading factors (SFs) and bandwidths (BWs). First, principles and properties of LoRa modulation and demodulation in discrete-time domain are presented, followed by theoretical analysis of the interference. Extensive simulation was performed to characterize the effect of interference on both detection signal-to-interference ratio (SIR) and the bit-error rate (BER) performance of the desired signals. Results demonstrate that the effect of interference is very serious if the desired and interfering signals have the same chirp rate (even though they might have different spreading factors and bandwidths), while it can be practically ignored for all other cases.**

I. Introduction

Recent years have seen wide acceptance of the Internet-of-Things (IoT) paradigm as the path forward for integrating digital devices into our society. This paradigm has the potential to enable communication between nearly any device and the Internet.

With the number of integrated devices already in the billions and steadily rising, two of the main constraints for an interconnected society are power usage and spectral efficiency. Many IoT devices are low data-rate devices that do not communicate continuously. For these devices, low power wide area networks (LPWANs) are conceived as solutions for connecting them in a manner such that they are resource efficient within the IoT paradigm.

LoRaWAN is an open-standard medium access control (MAC) layer protocol being developed by the LoRa Alliance [1] that works with both LoRa and frequency-shift keying (FSK) modulations. LoRa modulation is a patented modulation scheme developed by SemTech. It has many characteristics that make it well-suited for LPWAN technology, such as being Doppler and multipath/fading resistant as well as having low power requirements for long range communication [2].

In LoRa modulation, the raw bit rate can be controlled through two parameters within recommended ranges: *spreading factor* (SF), which ranges from 7 to 12, and *bandwidth* (BW), which can be either 125, 250, or 500 kHz [1]. Varying these parameters gives LoRa signals a raw bit rate ranging from 0.3 to 27 kbps. Other parameters can be set to orthogonalize signals and improve reception, such as center frequency and coding rate (which ranges from 4/5 to 4/8).

One of the main concerns about LoRaWAN is its scalability, which is still under evaluation. What is known is that using different spreading factors in LoRa does not make the transmitted signals perfectly orthogonal [3]. This means that collisions between LoRa signals having different spreading factors and bandwidths can prevent reception of the desired signals. This fact was observed in [4] and [5], which offer differing values for co-channel rejection thresholds, although it will be shown later that the results in this paper agree with [5]. In [6], experiments are made regarding collisions between signals in the same channel with distinct and matching spreading factors which seems to confirm the orthogonality of LoRa signals with different spreading factors, but the effect of varying other parameters along with the spreading factors in collisions is not tested. Solutions have been discussed which can demodulate signals transmitted with the same spreading factor in the same channel [7], which may have a similar use in the circumstances discussed in this paper.

In this paper, a detailed description of the chirp spread spectrum (CSS) signal set and DFT-based detection for LoRa is given. Analysis of the interference in the DFT-based detection was done across many sets of signal parameters (SF, BW, and signal-to-noise ratio), as well as the bit-error rate of LoRa demodulation. The obtained results are in good agreement with what reported in [5] regarding the signal-to-interference ratio (SIR) thresholds. More importantly, it is shown that the interfering signals with the same chirp-rate as the desired signal cause very serious (unacceptable) degradation on the bit error rates.

II. Principles of LoRa Modulation and Demodulation

In order to analyze and understand the impact of interference in LoRa systems, the principles and important properties of CSS modulation and demodulation in the digital domain are described and discussed in this section.

A. CSS Signal Set

In chirp spread spectrum, a data symbol is encoded into a chirp, which is a sinusoid whose instantaneous frequency

978-1-7281-0319-8/19/$31.00 ©2019 IEEE

sweeps linearly through the bandwidth (denoted as BW, in Hz). Let f_c be the center (carrier) frequency in Hz and $T_{\rm sym}$ be the symbol duration, which is also the length of the chirp, in seconds. A chirp begins sweeping its frequency linearly starting at some value, and when the instantaneous frequency reaches the highest value, say $f_c + BW/2$, it wraps over and starts from the lowest frequency, $f_c - BW/2$, until the end of the chirp signal.

In a LoRa system, one symbol carries SF bits, where SF is also known as the spreading factor. It follows that the CSS signal set has $M = 2^{SF}$ different symbols, which are distinguished by M different chirps with different starting frequencies. The symbol duration is related to the bandwidth and spreading factor as $T_{\rm sym} = 2^{SF}/BW = M/BW$ (seconds). The chirp rate, i.e., the rate at which the instantaneous frequency changes over time, can be defined as

$$\mu = \frac{BW}{T_{\rm sym}} = \frac{(BW)^2}{M} \text{ (Hz/second).} \quad (1)$$

Thus, over the same bandwidth, the chirp rate decreases linearly with the size of the signal set M (also known as the modulation order). On the other hand, with the same modulation order M, the chirp rate increases quadratically with the bandwidth. More importantly, it is pointed out that different combinations of BW and M can lead to the same chirp rate.

To define the CSS signal set in *baseband*, i.e., $f_c = 0$Hz, start with a definition of the *basic* chirp, which is a chirp that starts at the lowest frequency $f_c - BW/2$, sweeps through the entire bandwidth then stops at the highest frequency $f_c + BW/2$. Specifically, the baseband basic chirp is defined as follows:

$$x_0(t) = \exp\left\{j2\pi\left(\frac{\mu t}{2} - \frac{BW}{2}\right)t\right\},\ t \in [0, T_{\rm sym}]. \quad (2)$$

The basic chirp is also assigned as symbol zero. The next symbol in the set, i.e., symbol 1, is obtained by *cyclically shifting* symbol zero by an amount of $\Delta_t = 1/BW$. In general, symbol m is obtained by *cyclically shifting* symbol zero by an amount of $m\Delta_t$. Thus the M-ary signal set is

$$x_m(t) = x_0(\text{mod}(t - m\Delta_t, T_{\rm sym})),\ t \in [0, T_{\rm sym}] \quad m = 0, \ldots, M-1. \quad (3)$$

It can be mathematically shown that the above is an orthogonal signal set. That is

$$\frac{1}{T_{\rm sym}}\int_0^{T_{\rm sym}} x_m(t)x_n^*(t)\mathrm{d}t = \delta(m-n).$$

Since continuous-time baseband CSS signals are band-limited to $BW/2$, one can sample $x_m(t)$ at a sampling rate of $F_{\rm samp} = BW$ without any loss of information. This gives a set of discrete-time baseband CSS signals. Specifically, the discrete-time basic CSS symbol (i.e., symbol zero) is:

$$\begin{aligned} x_0[n] &= x_0(t)\big|_{t=nT_{\rm samp}=nBW^{-1}} \\ &= \exp\left\{j2\pi\left(\frac{\frac{BW^2}{M}nBW^{-1}}{2} - \frac{BW}{2}\right)nBW^{-1}\right\} \\ &= \exp\left\{j2\pi\left(\frac{n^2}{2M} - \frac{n}{2}\right)\right\};\ n = 0, 1, \ldots, M-1. \end{aligned} \quad (4)$$

The above expression shows an important fact that the sample values of the discrete-time basic CSS symbol solely depend on the modulation order M. Other important properties of the discrete-time chirps are as follows:

(i) One discrete-time chirp contains exactly $M = 2^{SF}$ complex samples.

(ii) The mth discrete-time symbol (chirp) can be obtained by cyclically shifting the discrete-time basic chirp by m samples:

$$x_m[n] = x_m(t)\big|_{t=nT_{\rm samp}} = x_0[\text{mod}(n-m, M)] \quad (5)$$

(iii) The discrete-time basic chirp repeats itself after every M samples. As a consequence, one can also have $x_m[n] = x_0[n+m]$.

(iv) All discrete-time chirps are orthogonal to each other, i.e., $\frac{1}{M}\sum_{n=0}^{M-1} x_m[n]x_k^*[n] = \delta[m-k]$.

B. DFT-Based Detection of CSS Signals

Consider an additive white Gaussian noise (AWGN) channel. Then the continuous-time received signal in baseband over the first symbol duration is represented as

$$r(t) = x_m(t) + w(t),\ t \in [0, T_{\rm sym}] \quad (6)$$

where $x_m(t)$ is the transmitted chirp and $w(t)$ is circularly-symmetric complex Gaussian random process with power spectral density N_0 watts/sec/Hz. By sampling $r(t)$ with $F_{\rm samp} = BW$, one obtains the following discrete-time AWGN channel model:

$$r[n] = x_m[n] + w[n],\ n = 0, \ldots, M-1 \quad (7)$$

where $w[n]$ are i.i.d. $\mathcal{CN}(0, N_0)$. With this channel model, the so-called channel signal-to-noise ratio (SNR) is defined as $\text{SNR} = \frac{M}{MN_0} = \frac{1}{N_0}$. Since one symbol carries SF bits and has unit energy, the energy per bit is $E_b = 1/SF$ and $\frac{E_b}{N_0} = \frac{1}{SF \cdot N_0}$.

The DFT-based detection is based on the observation that multiplying any chirp with the complex conjugate of the basic chirp yields a sinusoid of a constant frequency. This is formally shown as follows:

$$\begin{aligned} v_m[n] &= x_m[n]x_0^*[n] \\ &= \exp\left\{j2\pi\left(\frac{(n+m)^2}{2M} - \frac{n+m}{2} - \frac{n^2}{2M} + \frac{n}{2}\right)\right\} \\ &= \underbrace{\exp\left\{j2\pi\left(\frac{m^2}{2M} - \frac{m}{2}\right)\right\}}_{\text{constant phase}}\underbrace{\exp\left\{\frac{j2\pi nm}{M}\right\}}_{\text{pure sinusoid}}. \end{aligned} \quad (8)$$

It can be seen that $v_m[n]$ is a pure complex sinusoid at frequency of m/M (cycles/sample). Thus, if an M-point DFT is performed on $\{v_m[n]\}_{n=0}^{M-1}$, one obtains:

$$\begin{aligned} V_m[k] &= \sum_{n=0}^{M-1} v_m[n] \exp\left\{\frac{-j2\pi nk}{M}\right\} \\ &= \exp\left\{j2\pi\left(\frac{m^2}{2M} - \frac{m}{2}\right)\right\} \\ &\times \sum_{n=0}^{M-1} \exp\left\{\frac{j2\pi n(m-k)}{M}\right\},\ k = 0, \ldots, M-1 \\ &= \begin{cases} M \exp\left\{j2\pi\left(\frac{m^2}{2M} - \frac{m}{2}\right)\right\}, \text{ if } k = m \\ 0, \text{ if } k \neq m \end{cases} \end{aligned} \tag{9}$$

Including the noise component $w[n]$, the output of the DFT becomes:

$$\begin{aligned} R[k] &= V_m[k] + W[k] \\ &= \begin{cases} M \exp\left\{j2\pi\left(\frac{m^2}{2M} - \frac{m}{2}\right)\right\} + W[m], \text{ if } k = m \\ W[k], \text{ if } k \neq m \end{cases} \end{aligned} \tag{10}$$

where $W[k]$, $k = 0, \ldots, M-1$, is the DFT of $w[n]x_0^*[n]$. It can be shown that $W[k]$ are i.i.d. $\mathcal{CN}(0, MN_0)$. Finally, the DFT-based detection is performed on $R[k]$ as follows:

$$m = \arg\{\max_{0 \leq k \leq M-1} |R[k]|\}. \tag{11}$$

III. Interference Analysis

In LoRaWAN, different end devices are allowed to communicate simultaneously to the gateway using different spreading factors, bandwidths and channels (carrier frequencies). In this section, the interference caused by one device to the other when they transmit on the same channel (i.e., same carrier frequency) is analyzed. To this end, consider the following received signal:

$$\widehat{r}(t) = x_m(t) + \kappa y(t) + w(t) \tag{12}$$

where $x_m(t)$ is the desired signal, $y(t)$ is a CSS signal sent by a non-desired (interfering) device, κ models the attenuation on the interfering signal relative to the desired signal, and $w(t)$ is the usual AWGN.

As before, the desired signal has duration $T_{\text{sym}} = M/BW$, whereas the duration of the interfering signal is $\widehat{T}_{\text{sym}} = \widehat{M}/\widehat{BW}$. In general, $y(t)$ is not necessarily synchronized to $x_m(t)$ at the symbol boundary $t = 0$ and there is a random delay $\tau \in [-\widehat{T}_{\text{sym}}, \widehat{T}_{\text{sym}}]$ between the two waveforms. Moreover, depending on the values of M, BW, $\widehat{M}$, $\widehat{BW}$, the duration of the interfering CSS symbol can be longer or shorter than T_{sym}. There are then two possibilities to consider:

(1) If $\widehat{T}_{\text{sym}} \geq T_{\text{sym}}$, then portions of two CSS symbols in $y(t)$ interfere with the desired signal $x(t)$. As such, it suffices to represent $y(t)$ as

$$y(t) = \sum_{q=0}^{1} \widehat{x}_{m_q}(t - q\widehat{T}_{\text{sym}} - \tau)$$

For the synchronous case that $\tau = 0$, then the m_0 symbol in $y(t)$ defined above does not overlap the desired signal.

(2) If $\widehat{T}_{\text{sym}} < T_{\text{sym}}$, say $T_{\text{sym}}/\widehat{T}_{\text{sym}} = Q$, then it is necessary to consider $y(t)$ as made up of $Q-1$ complete CSS symbols, along with portions of two symbols at the beginning and end. That is,

$$y(t) = \sum_{q=0}^{Q} \widehat{x}_{m_q}(t - q\widehat{T}_{\text{sym}} - \tau)$$

For the synchronous case that $\tau = 0$, then the m_0 and m_Q symbols in $y(t)$ defined above do not overlap the desired signal.

To detect the CSS symbol of the desired user, $\widehat{r}(t)$ is sampled with $F_{\text{samp}} = BW$. Ignoring AWGN (to focus on interference), the received samples are:

$$\begin{aligned} \widehat{r}[n] &= \widehat{r}(t)\big|_{t=nT_{\text{samp}}} \\ &= x_m[n] + \kappa y[n],\ n = 0, 1, \ldots, M-1 \end{aligned} \tag{13}$$

where $y[n] = y(t)\big|_{t=nT_{\text{samp}}}$. The de-chirped signal then becomes:

$$\widehat{v}[n] = \widehat{r}[n]x_0^*[n] = (x_m[n] + \kappa y[n])x_0^*[n] = v_m[n] + \kappa i[n] \tag{14}$$

where $v_m[n]$ is given as in (8) and $i[n] = y[n]x_0^*[n]$. Following the same analysis as in (8), it can be shown that the de-chirped interfering signal is given by:

$$\begin{aligned} i[n] = \sum_{q=0}^{Q} \Bigg[\exp\Bigg\{ j2\pi \Bigg(& \frac{\left(\frac{\widehat{BW}}{BW}n + m_q - \widehat{BW}\tau\right)^2}{2\widehat{M}} \\ & - \frac{\frac{\widehat{BW}}{BW}n + m_q - \widehat{BW}\tau}{2} - \frac{n^2}{2M} + \frac{n}{2} \Bigg) \Bigg\} \Bigg] \end{aligned} \tag{15}$$

It is simple to check that $i[n] \neq 0$ for all combinations of $\{SF, \widehat{SF}, BW, \widehat{BW}\}$ where $SF, \widehat{SF} \in \{7, 8, \ldots, 12\}$ and $BW, \widehat{BW} \in \{125\text{kHz}, 250\text{kHz}, 500\text{kHz}\}$ and whenever $\kappa \neq 0$.

Computing the DFT of $\widehat{v}[n]$ results in:

$$\widehat{V}[k] = \begin{cases} M \exp\left\{j2\pi\left(\frac{m^2}{2M} - \frac{m}{2}\right)\right\} + I[m], \text{ if } k = m \\ I[k], \quad \text{if } k \neq m \end{cases} \tag{16}$$

To quantify the effect of interference on the detection of the desired signal, define the *detection* signal-to-interference ratio (SIR) as follows:

$$\text{SIR}_{\text{det}} = \frac{M^2}{\kappa^2 E\{|I[k_p]|^2\}}, \tag{17}$$

where k_p is the frequency bin corresponding to the peak of the interfering signal and the expectation operation is over all symbols m_q and the uniform random delay τ (for the case of asynchronous interference).

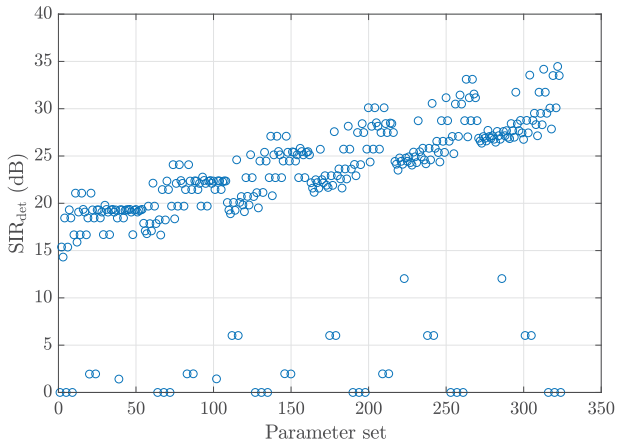

Fig. 1: Average SIR_{det} for varying sets of parameters: Synchronous interference.

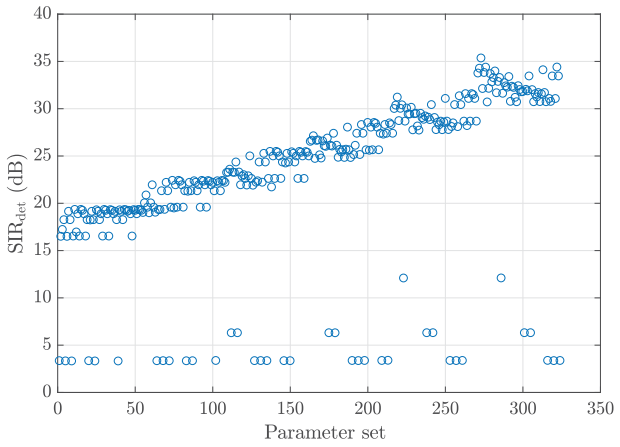

Fig. 2: Average SIR_{det} for varying sets of parameters: Asynchronous interference with uniform random delay.

IV. Numerical Results and Discussion

A CSS system with one desired signal and one interfering signal was simulated in MATLAB with $\kappa = 1$, i.e., the desired and interfering signals have the same power. For each transmission, 10 random data symbols were generated for the desired signal before being added to an interfering signal consisting of enough randomly generated data symbols to fully overlap the desired signal.

A. Effect of Interference on the detection SIR

The detection SIR in (17) was first examined for the case of synchronized interference (i.e., $\tau = 0$). Specifically, SIR_{det} was calculated as the average of 10^4 runs for each set of parameters $\{SF, \widehat{SF}, BW, \widehat{BW}\}$, where $SF, \widehat{SF} \in \{7, 8, \ldots, 12\}$ and $BW, \widehat{BW} \in \{125\text{kHz}, 250\text{kHz}, 500\text{kHz}\}$. The results of this simulation are plotted in Fig. 1, where the horizontal axis represents the index set of parameters (the sets go through each value of $\widehat{BW}$ first, then BW, $\widehat{SF}$, and finally SF).

Considered next in the more realistic situation in which the interfering signal is infinitely long and has random delay τ, where $0 \leq \tau \leq \widehat{T}_{\text{sym}}$ so that it always overlaps with the desired signal. Fig. 2 plots SIR_{det} obtained by averaging over 10^4 runs for each combination of $\{SF, \widehat{SF}, BW, \widehat{BW}\}$ where $SF, \widehat{SF} \in \{7, 8, \ldots, 12\}$ and $BW, \widehat{BW} \in \{125\text{kHz}, 250\text{kHz}, 500\text{kHz}\}$.

It can be seen from Figs. 1 and 2 that there are certain parameter sets resulting in noticeably lower SIR_{det} values than the rest. It turns out that these parameter sets are the ones where the interfering and desired signals have the same chirp rate, that is to say:

$$\frac{BW^2}{M} = \frac{\widehat{BW}^2}{\widehat{M}} \tag{18}$$

There are three cases that result in two signals having the same chirp rate:

1) $SF_x = SF_y$ and $BW_x = BW_y$
2) $SF_x = SF_y + 2$ and $BW_x = 2BW_y$
3) $SF_x = SF_y + 4$ and $BW_x = 4BW_y$

where x and y refer to two different signals.

Examining Fig. 1 in detail reveals that there are five different SIR_{det} levels for these signals: the lowest being the case where the desired and interfering signals have the same SF and BW, the next level (of which there are only two points) is where the interfering signal BW is 4 times the desired signal BW, the middle level is where the interfering signal BW is 2 times the desired signal BW, the fourth level is where the desired signal BW is 2 times the interfering signal BW, the highest level is where the desired signal BW is 4 times the interfering signal BW.

In Fig. 2, three levels can be seen for the same-chirp-rate sets: the lowest level corresponds to sets where the desired signal either has the same or lower SF and BW as compared to the interference; the middle level corresponds to sets where $SF = \widehat{SF}+2$ and $BW = 2\widehat{BW}$; the highest level corresponds to sets where $SF = \widehat{SF} + 4$ and $BW = 4\widehat{BW}$.

B. Effect of Interference on BER Performance

To examine the effect of interference on the detection performance with different spreading factors and bandwidths, the bit-error rate (BER) was first obtained for signals with AWGN but no interference. In the simulation, frames of 10 random data symbols were sent 1.5×10^5 times for spreading factors 8 to 12 ($BW = 125$ kHz for all). The BER curves versus SNR are plotted as solid lines in Fig. 3 for this case.

To observe the effect of interference on the BER, an interfering signal with $SF = 10$ and $BW = 250\text{kHz}$ was added. The resulting BER curves are plotted as dashed lines in Fig. 3. It can be clearly seen that the effect of the interfering signal is not significant except when its chirp rate matches the chirp rate of the desired signal. For such a case, the BER curve flattens out significantly and at much higher error rates.

In order to see the effects of interference on the BER for all combinations of SF and BW of the desired and interfering signals, Table I was generated, which shows the SIR thresholds, which are the SIR values at which the BER is ≤ 0.01, for every combination of $SF, \widehat{SF} \in \{7, 8, \ldots, 12\}$ and $BW, \widehat{BW} \in \{125\text{kHz}, 250\text{kHz}, 500\text{kHz}\}$. It is pointed

TABLE I: SIR thresholds in dB (for BER < 0.01).

SF \ $\widehat{SF}$	7	8	9	10	11	12
7	0	-10	-11	-12	-13	-13
8	-12	0	-12	-13	-15	-16
9	-15	-15	0	-15	-16	-18
10	-18	-18	-18	0	-18	-19
11	-20	-21	-21	-20	0	-21
12	-23	-23	-23	-24	-23	0

(a) $BW = 125$kHz, $\widehat{BW} = 125$kHz

SF \ $\widehat{SF}$	7	8	9	10	11	12
7	-10	-10	0	-10	-12	-13
8	-12	-13	-13	0	-13	-15
9	-15	-15	-15	-16	0	-16
10	-17	-18	-18	-18	-19	0
11	-20	-20	-20	-21	-21	-22
12	-23	-23	-23	-23	-24	-24

(b) $BW = 125$kHz, $\widehat{BW} = 250$kHz

SF \ $\widehat{SF}$	7	8	9	10	11	12
7	-9	-10	-10	-11	1	-11
8	-12	-12	-13	-13	-14	0
9	-14	-15	-15	-15	-16	-17
10	-17	-17	-17	-18	-19	-19
11	-20	-20	-20	-20	-21	-21
12	-23	-23	-23	-23	-23	-23

(c) $BW = 125$kHz, $\widehat{BW} = 500$kHz

SF \ $\widehat{SF}$	7	8	9	10	11	12
7	-10	-11	-12	-13	-13	-13
8	-11	-13	-14	-15	-16	-16
9	-5	-14	-15	-16	-18	-19
10	-17	-5	-17	-18	-19	-20
11	-20	-20	-5	-20	-21	-22
12	-23	-23	-23	-6	-23	-24

(d) $BW = 250$kHz, $\widehat{BW} = 125$kHz

SF \ $\widehat{SF}$	7	8	9	10	11	12
7	0	-10	-11	-12	-13	-13
8	-12	0	-12	-14	-15	-16
9	-15	-15	0	-15	-17	-18
10	-18	-18	-18	0	-18	-19
11	-20	-21	-21	-20	0	-21
12	-23	-23	-23	-24	-23	0

(e) $BW = 250$kHz, $\widehat{BW} = 250$kHz

SF \ $\widehat{SF}$	7	8	9	10	11	12
7	-10	-10	0	-10	-12	-13
8	-12	-13	-13	0	-13	-15
9	-15	-15	-15	-16	0	-16
10	-17	-18	-18	-18	-19	0
11	-20	-20	-20	-21	-21	-22
12	-23	-23	-23	-23	-24	-24

(f) $BW = 250$kHz, $\widehat{BW} = 500$kHz

SF \ $\widehat{SF}$	7	8	9	10	11	12
7	-11	-12	-13	-13	-13	-13
8	-13	-14	-15	-16	-16	-16
9	-16	-16	-17	-17	-19	-19
10	-17	-19	-19	-20	-21	-22
11	-11	-20	-21	-22	-23	-23
12	-23	-11	-23	-24	-25	-26

(g) $BW = 500$kHz, $\widehat{BW} = 125$kHz

SF \ $\widehat{SF}$	7	8	9	10	11	12
7	-10	-11	-12	-13	-13	-13
8	-11	-13	-14	-15	-16	-16
9	-5	-14	-15	-16	-18	-19
10	-17	-5	-17	-18	-19	-20
11	-20	-20	-5	-20	-21	-22
12	-23	-23	-23	-6	-23	-24

(h) $BW = 500$kHz, $\widehat{BW} = 250$kHz

SF \ $\widehat{SF}$	7	8	9	10	11	12
7	0	-10	-11	-12	-13	-13
8	-12	0	-12	-14	-15	-16
9	-15	-15	0	-15	-17	-18
10	-18	-18	-18	0	-18	-19
11	-20	-21	-21	-20	0	-21
12	-23	-23	-23	-24	-23	0

(i) $BW = 500$kHz, $\widehat{BW} = 500$kHz

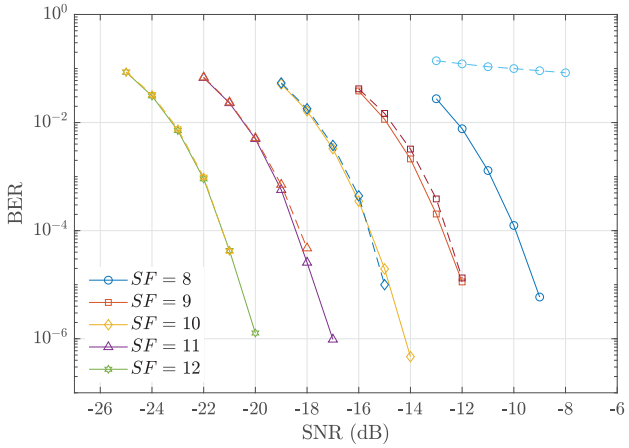

Fig. 3: BER versus SNR. Solid lines are for the case of AWGN only (no interference). Dashed lines are obtained with added asynchronous interfering signal (interfering signal has $SF = 10$ and $BW = 250$kHz, whereas the bandwidth of the desired signals is 125kHz).

out that Tables I (a), (e) and (i) contain thresholds that are nearly identical to each other, and very similar to the values reported in Table 1 in [5]. The difference (1 to 2 dB) is perhaps because channel coding is not implemented in our simulation. It can be seen in Tables I (d) and (h) that there is a 5 to 6 dB decrease in the SIR threshold for same-chirp-rate signals and when the desired signal is one bandwidth setting higher than the interference's bandwidth. Likewise, Table I (g) shows that there is an 11 dB decrease in the SIR threshold when the desired bandwidth is two settings higher than the interference's bandwidth.

V. Conclusions

This paper has demonstrated that interfering signals from other LoRa devices cause significant errors in reception of the desired signal if they have the same chirp rate. This effect causes signals with the same chirp-rate to have an SIR threshold that is the same as signals with the same SF and BW, but for each factor of 2 the desired signal BW is over the interfering signal BW this threshold decreases by 5 to 6 dB. This finding suggests that signals with poorer channel quality should switch to higher BW settings before changing SF if there are signals in the channel with the same chirp rate in order to reduce the effect of collisions.

Acknowledgement

This work was supported by an NSERC/Cisco IRC in Low-Power Wireless Access for Sensor Networks.

References

[1] L. Alliance, "LoRaWAN Specification v1.1," 2017.
[2] SemTech, "AN1200.22: LoRa Modulation Basics," May 2015.
[3] B. Reynders and S. Pollin, "Chirp spread spectrum as a modulation technique for long range communication," in *IEEE Symp. on Commun. and Veh. Technol.*, pp. 1–5, Nov. 2016.
[4] C. Goursaud and J. Gorce, "Dedicated networks for IoT: PHY/MAC state of the art and challenges," *EAI Endored Transactions on the Internet of Things*, vol. 1, pp. 1–11, Oct. 2015.
[5] D. Croce, M. Gucciardo, S. Mangione, G. Santaromita, and I. Tinnirello, "Impact of LoRa Imperfect Orthogonality: Analysis of Link-Level Performance," *IEEE Commun. Letters*, vol. 22, pp. 796–799, Apr. 2018.
[6] J. C. Liando, A. Gamage, A. W. Tengourtius, and M. Li, "Known and unknown facts of lora: Experiences from a large-scale measurement study," *ACM Trans. Sen. Netw.*, vol. 15, pp. 16:1–16:35, Mar. 2018.
[7] R. Eletreby, D. Zhang, S. Kumar, and O. Yağan, "Empowering low-power wide area networks in urban settings," in *Proceedings of the Conference of the ACM Special Interest Group on Data Communication*, pp. 309–321, Aug. 2017.